Research Square

Preprints are preliminary reports that have not undergone peer review.
They should not be considered conclusive, used to inform clinical practice,
or referenced by the media as validated information.

Energy-based plastic design and seismic evaluation of doubly buckling-restrained knee-braced frames

Piseth Doung

piseth@itc.edu.kh

Institute of Technology of Cambodia

Kimtong Theng

Institute of Technology of Cambodia

Leangheng Chea

Institute of Technology of Cambodia

Sutat Leelataviwat

King Mongkut's University of Technology Thonburi

Research Article

Keywords: Capacity design, D-BRKBF, energy-based plastic design, knee-braced frames

Posted Date: October 28th, 2026

DOI: https://doi.org/10.21203/rs.3.rs-11487370/v1

License: This work is licensed under a Creative Commons Attribution 4.0 International License.
Read Full License

Additional Declarations: No competing interests reported.

Energy-based plastic design and seismic evaluation of doubly buckling-restrained knee-braced frames

Piseth Doung[1,2], Kimtong Theng[1], Leangheng Chea[2] and Sutat Leelataviwat[3]

Abstract
This paper presents the energy-based plastic design and seismic performance evaluation of steel doubly buckling-restrained knee-braced frames. The study aims to propose a structural design method, referred to as energy-based plastic design, for these framing systems, and to verify their seismic performance through nonlinear static pushover and dynamic time-history analyses. First, four frames with 3-, 6-, 9-, and 12-story configurations were designed using the energy-based plastic design and capacity design approaches for hazard levels corresponding to the design basis earthquake (DBE) and the maximum considered earthquake (MCE). Second, nonlinear static pushover and dynamic time-history analyses were conducted to evaluate the inelastic behavior of the frames, including capacity curves, yield activity, and maximum inter-story drifts. The pushover analysis estimated the monotonic capacity in terms of roof drift and identified the inelastic behavior of the structural members. The dynamic analyses used 22 pairs of ground motions scaled to the DBE and MCE levels. The yield activity and inter-story drifts were identified, compared, and discussed. The results showed that the low- and medium-rise frames designed using this approach satisfied the strength and deformation requirements, ensuring a controlled yield mechanism within the target drifts of 2% and 3% for the DBE and MCE levels, respectively. For the 9- and 12-story frames, however, the yield mechanism was not fully developed because the column bases did not yield within the target drift limits. Further studies on high-rise systems above six stories should therefore consider higher-mode effects on the yield mechanism and cumulative seismic behavior.

Keywords: Capacity design, D-BRKBF, energy-based plastic design, knee-braced frames

---

Correspondence to: Piseth Doung
Email: piseth@itc.edu.kh

[1] Department of Civil Engineering, Institute of Technology of Cambodia, Phnom Penh 120404, Cambodia

[2] Research and Innovation Center, Institute of Technology of Cambodia, Phnom Penh 120404, Cambodia

[3] Department of Civil Engineering, King Mongkut's University of Technology Thonburi, Bangkok 10140, Thailand

Introduction

Many works have gone into developing seismic force-resisting frames that remain safe and resilient in strong earthquakes. Such systems need adequate strength, stiffness, and ductility while maintaining structural safety and minimizing damage to structural components. Conventional braced systems, for example concentrically braced frames (CBFs) and eccentrically braced frames (EBFs), are widely recognized for providing their high lateral resistance and excellent energy dissipation. However, these systems often restrict the architectural and mechanical layouts of a building, thereby limiting the usable floor space. The knee-braced frame (KBF) system utilizes short braces located close to the beam-column connection region, allowing greater flexibility for architectural planning (Kim and Seo, 2003; Leelataviwat et al., 2011; Piseth Doung, 2016). In recent years, KBFs for seismic use have been examined in numerous experimental and analytical studies (Eknara Junda, 2011; Leelataviwat et al., 2011, 2019; Wongpakdee et al., 2014; Yang et al., 2014; Piseth Doung, 2016; Junda et al., 2018), which showed that the system delivers high strength together with moderate stiffness and ductility.

Kim and Seo (2003) first put forward a new knee-braced configuration, the "doubly knee-braced frame," and proposed a seismic design approach for it. Using double knee braces significantly enhanced both the strength and the stiffness compared with the conventional singly knee-braced system. Gao et al. (2022) later carried out an experimental study on doubly knee-braced connections with buckling-restrained braces (BRBs) in steel frames. Their study demonstrated that the doubly knee-braced frame system exhibited superior hysteretic energy dissipation compared with the singly knee-braced frame system. Doubly knee-braced-type connections have also been used to enhance the seismic performance of semi-rigid steel frames (Li et al., 2021). Based on these developments, the doubly buckling-restrained knee-braced frame (D-BRKBF) system is proposed in this study. The D-BRKBF incorporates BRBs as knee-bracing members at the beam-column connection regions, above and below each floor level, thereby preserving open bay spaces for architectural use. This structural configuration provides better energy dissipation and a more uniform distribution of inelastic demand, and it helps facilitate the repair and replacement of damaged components following an earthquake. To design the proposed structural system, an energy-based plastic design (EBPD) methodology was used to determine the design base shear for a specified seismic hazard level. EBPD is derived from the conventional performance-based plastic design (PBPD) method (Leelataviwat, 1998; Lee and Goel, 2001; Chao and Goel, 2006; Goel et al., 2010; Liao and Goel, 2012; Leelataviwat et al., 2021), which has been applied for various structural systems, including KBFs. The method is mainly based on the principle of energy balance. The EBPD procedure involves preselecting the target yield mechanism and design drift and subsequently pushing and reversing the structure under monotonic loading (Goel and Furukawa, 2009; Chea et al., 2025a, b). This procedure enables the equivalent hysteretic behavior of the structural system to be represented.

In this study, the EBPD method is applied to the design of D-BRKBF systems equipped with BRBs. Four prototype structures with 3, 6, 9, and 12 stories were designed and evaluated at the design basis earthquake (DBE) and maximum considered earthquake (MCE) hazard levels. A capacity design approach was adopted to determine the internal forces and to design the BRBs, beams, and columns. To evaluate the seismic performance, nonlinear static pushover (NSP) and nonlinear dynamic time-history (NDTH) analyses were carried out. Key performance parameters, including pushover capacity curves, inelastic response, and inter-story drifts, were examined. The deformation demands predicted from the NSP and NDTH analyses were then compared and discussed, along with the limitations of the proposed evaluation approach.

Energy-based plastic design method

The energy-based plastic design (EBPD) method proposed in this study is a direct seismic design procedure for structural framing systems, in which a plastic mechanism and target drift levels are specified at the outset. It is based on an energy balance that equates the elastic energy supplied to the structure with the energy dissipated through plastic deformation in an equivalent structural system. The design seismic base shear follows from this balance concept. The foundation of this approach was first introduced by Housner (1956), which laid the groundwork for subsequent developments in energy-based seismic design. He showed that the energy needed to push an elastic-perfectly plastic single-degree-of-freedom (SDOF) system to a target displacement equals the elastic energy an earthquake delivers to that system. Based on this idea, the PBPD method was formulated and later applied to a range of structural systems. In PBPD, the plastic mechanism and the target drift associated with the fundamental vibration mode are predefined, and these are used to compute the design base shear for a specified seismic hazard level (Housner, 1956; Goel and Furukawa, 2009; Leelataviwat et al., 2009; Chea et al., 2025b, a).

Recent studies have extended the design methodology further to account for the cumulative seismic behavior of structural systems (Naiyana et al., 2023, 2025; Goudarzi et al., 2026). Naiyana et al. (2023, 2025) considered cumulative damage caused by hysteretic energy dissipation to evaluate the seismic performance of low-rise and tall knee-braced frames. Consequently, the lateral force distributions were adjusted to reflect cumulative damage

effects. Similarly, Goudarzi et al. (2026) investigated the cumulative damage of reinforced concrete moment-resisting frames subjected to sequential earthquakes.

More recently, Leangheng et al. (2023) and Chea et al. (2025a, b) proposed modifications to the energy factors used in both the seismic design and the damage evaluation of steel moment-resisting frames. The energy factor is defined as the ratio of the plastic energy response to the elastic energy response of an equivalent SDOF system. Chea et al. (2025a, b) introduced two energy factors, γ_1 and γ_2, which represent the monotonic and hysteretic responses, respectively. The monotonic energy factor, γ_1, was obtained from an idealized elastic-perfectly plastic force–deformation relationship of the structural system, as illustrated in Fig. 1.

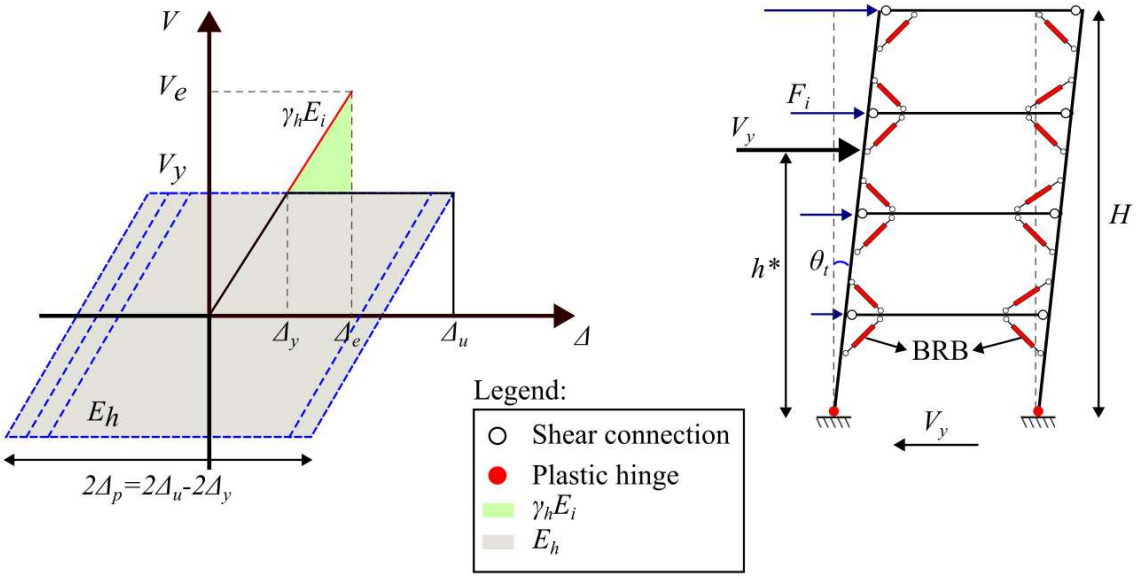

Fig. 1 EBPD concept (Leangheng et al., 2023)

Based on the work-energy principle, the concept of energy balance can be expressed as follows:

$$E_e + E_p = \gamma E_i \tag{1}$$

where γ and E_i denote the energy modification factor and the input seismic energy of an equivalent elastic system, respectively. Alıcı and Sucuoğlu (2016) suggested the expression for the input seismic energy by considering the correlation between the equivalent velocity (V_{eq}) and the pseudo-velocity S_v, which can be expressed as:

$$E_i = \frac{1}{2}\eta^2 M {S_v}^2 \tag{2}$$

where η is the ratio of the equivalent velocity (V_{eq}) to pseudo-velocity (S_v) and M is the total mass of the structure. An empirical expression for estimating the velocity ratio, η, was proposed as a function of the fundamental period of the equivalent SDOF system and dimensionless coefficients:

$$\eta = \frac{V_{eq}}{S_v} = a.e^{-bT} + c \tag{3}$$

where T is the fundamental period of the equivalent SDOF system, and a, b, and c are empirical coefficients. S_v denotes the pseudo-velocity, which is expressed in terms of the pseudo-acceleration as $S_v = S_aT/2\pi$. The values of the velocity ratio, η, are shown in Fig. 2.

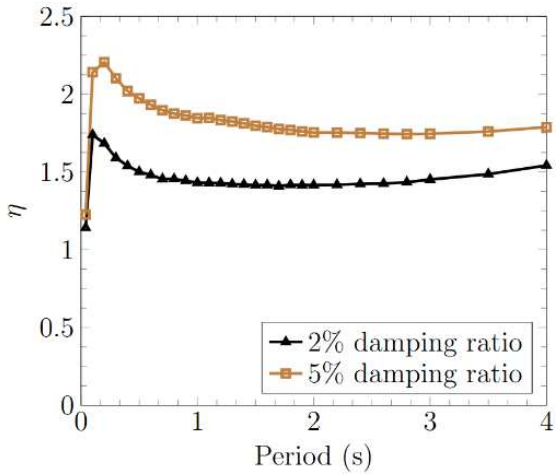

Fig. 2 Values of the velocity ratio, η, by Alıcı and Sucuoğlu (2016)

Eq. (1) represents the monotonic force-deformation behavior of an equivalent SDOF system. In this study, however, the hysteretic behavior of the structure is assumed to be a stable parallelogram-shaped hysteresis loop, and the total hysteretic energy is calculated as the area enclosed by the loop. To account for this hysteretic behavior, a hysteretic energy factor, γ_h, is introduced, and the work-energy principle becomes:

$$E_h = \gamma_h E_i \tag{4}$$

The hysteretic energy factor, γ_h, was derived through a mathematical interpretation from the areas that represent the stable hysteretic energy response, and can be expressed as:

$$\gamma_h = \frac{E_h}{E_i} = \frac{4V_y\Delta_p}{\frac{1}{2}\eta^2 V_e\Delta_e} = \frac{8V_y(\Delta_u - \Delta_y)}{\eta^2 V_e\Delta_e} = \frac{8\left(\frac{\Delta_u}{\Delta_y} - 1\right)}{\eta^2 \frac{V_e}{V_y}\frac{\Delta_e}{\Delta_y}} \tag{5}$$

Taking $R_\mu = V_e/V_y = \Delta_e/\Delta_y$ and $\mu = \Delta_u/\Delta_y$ as the strength reduction and the ductility factors, respectively, the hysteretic energy factor, γ_h, can be rewritten as:

$$\gamma_h = \frac{8(\mu - 1)}{\eta^2 {R_\mu}^2} \tag{6}$$

The R_μ-μ-T relationship proposed by Newmark and Hall (1982) can be used to establish the relationship between the hysteretic energy factor (γ_2), the strength reduction factor (R_μ), the ductility factor (μ), and the fundamental period (T). These relationships are summarized in Table 1 below. The variations of the hysteretic energy factor for different damping ratios are illustrated in Fig. 3.

Table 1 Hysteretic energy factor (γ_h)

Period (T)	Strength reduction factor (R_μ)	Energy factor (γ_h)
$0 \le T < \frac{T_1}{10}$	$R_\mu = 1$	$\gamma_h = \frac{8(\mu-1)}{\eta^2}$
$\frac{T_1}{10} \le T < \frac{T_1}{4}$	$R_\mu = \sqrt{2\mu-1}\left[\frac{T_1}{4T}\right]^{2.513\log\left(\frac{1}{\sqrt{2\mu-1}}\right)}$	$\gamma_h = \frac{8(\mu-1)}{\eta^2(2\mu-1)\left[\frac{T_1}{4T}\right]^{5.026\log\left(\frac{1}{\sqrt{2\mu-1}}\right)}}$
$\frac{T_1}{4} \le T < T_1'$	$R_\mu = \sqrt{2\mu-1}$	$\gamma_h = \frac{8(\mu-1)}{\eta^2(2\mu-1)}$

$T_1' \leq T < T_1$	$R_\mu = \frac{T_\mu}{T_1}$	$\gamma_h = \frac{8(\mu-1)}{\eta^2 T_\mu^2} T_1^2$
$T_1 \leq T$	$R_\mu = \mu$	$\gamma_h = \frac{8(\mu-1)}{\eta^2 \mu^2}$

where T_1=0.57 s and $T_1'=\sqrt{2\mu\text{-}1}/\mu$

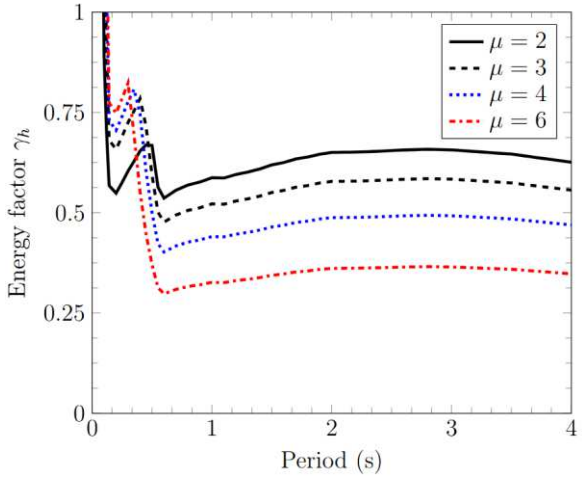

Fig. 3 Energy factor relationship specified for 5% damping ratio

To obtain the design base shear, the energy balance expressed in Eq. (1) can be rewritten using the concept illustrated in Fig. 1 as:

$$4V_y\Delta_p = \gamma_h \frac{1}{2}\eta^2 M {S_v}^2 \tag{7}$$

where Δ_p is the plastic displacement. By substituting $\Delta_p = h^*\theta_p$, $M = W/g$, and $S_v = S_a T/(2\pi)$ into Eq. (7) gives the design base shear of the system as:

$$\frac{V_y}{W} = \frac{\gamma_h \eta^2 \left(\frac{S_a T}{2\pi}\right)^2}{8h^*\theta_p g} \tag{8}$$

where h^*, θ_p, and g denote the height of the resultant lateral force for the plastic response of the equivalent SDOF system, the plastic drift ratio, and the gravitational acceleration, respectively.

Energy-Based Plastic Design of D-BRKBFs

Lateral force distribution

The energy-based plastic design (EBPD) of a doubly buckling-restrained knee-braced frame (D-BRKBF) relies on two main design inputs: a preselected yield mechanism and a target drift that corresponds to a given seismic hazard level. The procedure begins by selecting the intended yield mechanism and a target drift while preventing premature yielding of non-designated structural members. In the D-BRKBF system, the BRBs and columns are the members that yield, while the beams are designed to remain elastic. Plastic hinges due to bending are assumed to form at the column bases. The EBPD procedure controls the average drift of the D-BRKBF system to minimize structural and non-structural damage during earthquakes. Design guidelines such as ASCE/SEI 7-16 (ASCE/SEI, 2016) and the PEER Tall Building Initiative (PEER, 2010) specify inter-story drift limits for different hazard levels and performance objectives. Target drift ratios are usually 2% for the design basis earthquake (DBE) level and 3% for the maximum considered earthquake (MCE) level. The plastic drift ratio of the structure can be calculated as follows:

$$\theta_p = \theta_t - \theta_y \tag{9}$$

where θ_y and θ_t denote the yield and target drift ratios, respectively.

The design of a D-BRKBF requires sufficient strength to ensure that the structural deformation remains within the target drift limits. The lateral resistance of the frame is primarily provided by the plastic behavior of the BRBs and the column bases. Accordingly, the BRBs and column bases are designated as the primary yielding components. The required strengths of the BRBs, beams, and columns are determined using the capacity design approach. A key step in the design procedure is the determination of the lateral force distribution based on the intended inelastic behavior of the structure. The lateral force distribution is calculated based on the PBPD method developed by Lee and Goel (2001), and latest updated for KBFs by Naiyana et al. (2025), to ensure that the designed structure develops the predefined yield mechanism while maintaining structural stability. The lateral force applied at floor level i is expressed as:

$$F_i = \lambda_i V_y \tag{10}$$

where λ_i is the lateral force distribution factor at floor level i, which is given by

$$\lambda_i = (\beta_i - \beta_{i+1}) \left(\frac{w_n h_n}{\sum_{j=1}^{n} w_j h_j} \right)^{0.75T^{-0.2}} \tag{11}$$

where w_n and w_j denote the seismic weights of the structure at the top level and floor level j, respectively. The parameters h_j and h_n express the heights of level j and the roof level measured from the ground, respectively. The parameter β_i is the shear proportioning factor at floor level i, determined as:

$$\beta_i = \left(\frac{\sum_{j=i}^{n} w_j h_j}{w_n h_n} \right)^{0.75T^{-0.2}} \tag{12}$$

The equivalent height, from the ground to the resultant of the lateral force distribution, is calculated as:

$$h^* = \frac{\sum_{i=1}^{n} F_i h_i}{V_y} \tag{13}$$

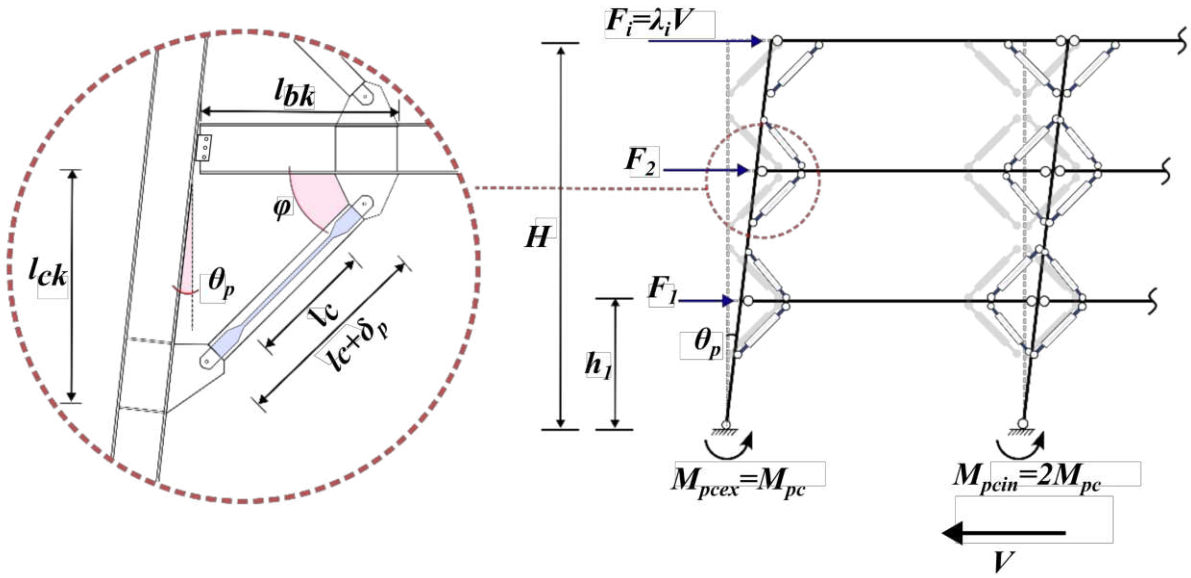

Fig. 4 Yield mechanism and deformation of the D-BRKBF

Design of BRBs

In the D-BRKBF system, the BRBs are designated as the primary yielding members and are intended to dissipate seismic energy through stable tension-compression plastic cycles. Using the yield mechanism illustrated in Fig. 4, the principle of virtual work was employed to determine the required axial strengths of the BRBs, represented

by $\beta_i P_{BRB}$. Assuming that the tensile and compressive strengths of the BRBs are approximately equal, the virtual work equation for an *N*-bay frame can be expressed as:

$$\sum_{i=1}^{n}(F_i h_i \theta_p) = \left(N \times 2M_{pc}\theta_p\right) + \sum_{i=1}^{n-1}\left(N \times 4\beta_i P_{BRB}\delta_p\right) + \left(N \times 2\beta_i P_{BRB}\delta_p\right) \tag{14}$$

where F_i is the lateral force at floor level i, θ_p denotes the plastic target drift, and β_i is the shear proportioning factor that accounts for the strength contribution of the BRBs at floor level i. The terms P_{BRB}, δ_p, and M_{pc} denote the required axial strength of the BRB, the plastic axial deformation of the BRB, and the required plastic moment capacity of the column base, respectively. *N* denotes the number of bays in the D-BRKBF system.

The required plastic moment capacity of the column base is determined based on the concept of preventing a soft-story mechanism. As illustrated in Fig. 4, the strength of the interior columns is assumed to be twice that of the exterior column ($M_{pcex} = M_{pc}$ and $M_{pcin} = 2M_{pc}$). Accordingly, the required plastic moment capacity of the exterior column base, M_{pc}, can then be determined as:

$$M_{pc} = \frac{1.1\left(\frac{V}{N}\right)h_1}{4} \tag{15}$$

where h_1 is the first-story height, and the factor of 1.1 represents the overstrength factor accounting for strain hardening at the plastic hinge of the column base. To determine the required BRB core size, the required axial strength of the BRB is calculated in accordance with the AISC Seismic Provisions (AISC, 2010), as follows:

$$\phi P_{ysc} = 0.9F_y A_{sc} = \beta_i P_{BRB} \tag{16}$$

where F_y and A_{sc} denote the yield strength and cross-sectional area of the BRB steel core, respectively.

Design of Beams and Columns

The required beam forces were determined using static equilibrium, ensuring that the beams remain elastic under the combined effects of gravity loads and the maximum forces generated by the BRBs, as illustrated in Fig. 5. According to the AISC Seismic Provisions (AISC, 2010), the cyclic behavior of BRBs, including the effects of strain hardening, is accounted for by the compression strength adjustment factor (β_0) and the strain-hardening adjustment factor (ω). Accordingly, the adjusted design strengths of a BRB are therefore expressed as follows:

In compression: $$P_{uc} = \omega\beta_0 R_y P_{ysc} \tag{17}$$

In tension: $$P_{ut} = \omega R_y P_{ysc} \tag{18}$$

where R_y is the material overstrength factor, while the values ω and β_0 are usually determined using test results obtained from BRBs with similar lengths, configurations, and restraining mechanisms to those used in the structure. In this study, approximate values of ω and β_0 were chosen as 1.4 and 1.1, respectively, in accordance with the tests conducted by Merritt et al. (2003). R_y can be chosen as 1.0 when the yield stress is determined from the coupon tests.

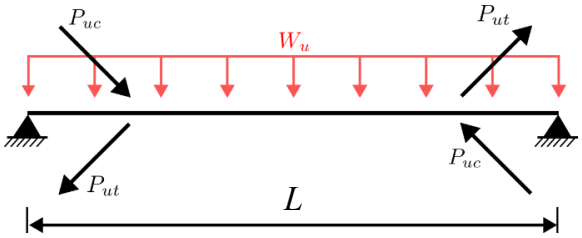

Fig. 5 Free-body diagram of the beam

The columns in the D-BRKBF system were designed as non-designated yielding members, except for their bases, which were permitted to yield to prevent a soft-story mechanism. The required column strengths were

determined by equating the equilibrium of all forces acting on the column using the "column tree" approach, as illustrated in Fig. 6. Accordingly, the total lateral force acting on a column can be expressed as follows:

For interior column:

$$F_{uin} = \frac{M_{pin} - \sum_{i=1}^{n}(P_{uc,i} + P_{ut,i})h_i' sin\varphi + \sum_{i=1}^{n-1}(P_{uc,i} + P_{ut,i})h_i'' sin\varphi + \sum_{i=1}^{n} N_{B,i}h_i}{\sum_{i=1}^{n} \alpha_i h_i} \quad (19)$$

For exterior rightmost column:

$$F_{uex(right)} = \frac{M_{pcex(right)} - \sum_{i=1}^{n} P_{uc,i}h_i' sin\varphi + \sum_{i=1}^{n-1} P_{ut,i}h_i'' sin\varphi - \sum_{i=1}^{n} N_{B,i}h_i}{\sum_{i=1}^{n} \alpha_i h_i} \quad (20)$$

For exterior leftmost column:

$$F_{uex(left)} = \frac{M_{pcex(left)} - \sum_{i=1}^{n} P_{ut,i}h_i' sin\varphi + \sum_{i=1}^{n-1} P_{uc,i}h_i'' sin\varphi + \sum_{i=1}^{n} N_{B,i}h_i}{\sum_{i=1}^{n} \alpha_i h_i} \quad (21)$$

where $N_{B,i}$ is the axial force in the beam at the floor level i, induced by the tension or compression force in the BRBs. The parameters h_i and h_i' denote the elevations of the lower and upper ends of the BRBs at floor level i, respectively. The terms $P_{ut,i}$ and $P_{uc,i}$ represent the adjusted nominal tensile and compressive strengths of the BRBs at the floor level i, respectively. The factor α_i is the lateral force distribution factor at floor level i, which is defined as:

$$\alpha_i = \frac{\beta_i - \beta_{i+1}}{\sum_{i=1}^{n}(\beta_i - \beta_{i+1})} \quad (22)$$

The lateral force acting on the column at floor level i can then be determined once the total lateral force and the corresponding distribution factor have been calculated, as follows:

$$F_{u,i} = \alpha_i F_u \quad (23)$$

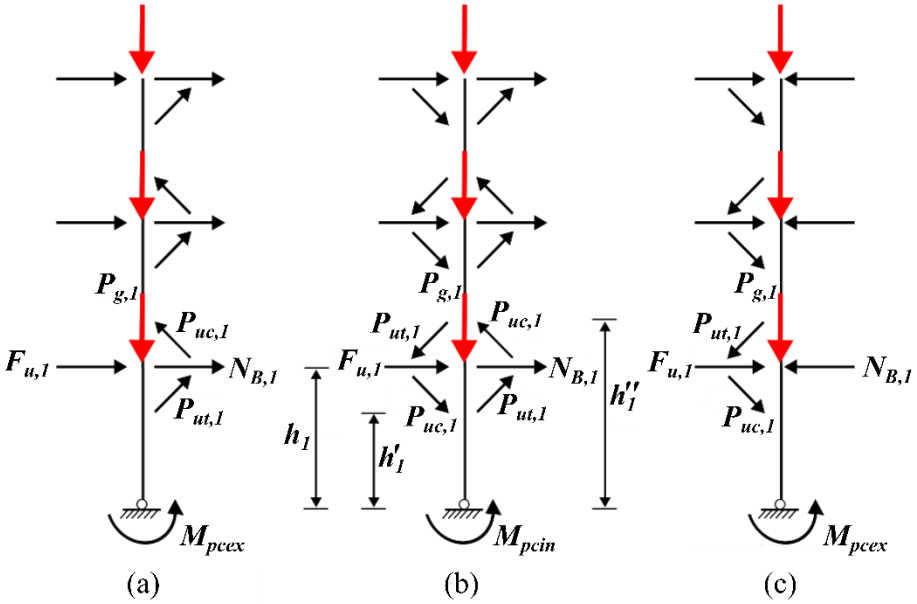

Fig. 6 Column tree analysis**: (a)** left-most column**, (b)** interior column**,** and **(c)** right-most column

Example D-BRKBF structures

Four D-BRKBF structures with 3, 6, 9, and 12 stories were designed using the EBPD method in this study. The building configuration followed the archetype structure adopted in an earlier study by Leelataviwat et al. (2011).

All buildings were assumed to have office occupancy. The floor plans and elevations of the study buildings are illustrated in Fig. 7. Each building consists of three bays in the North–South (N–S) direction and four bays in the East–West (E–W) direction. All stories have a uniform height of 3.96 m, and each bay has a span length of 9.14 m. The perimeter frames in the E–W direction were assumed to resist lateral loads with a conventional bracing system, while the perimeter frames in the N–S direction were designed as D-BRKBF systems and are the focus of this study. The interior frames were designed to carry gravity loads only.

The buildings were designed for a Site Class D soil profile, with spectral accelerations of $S_s = 1.5g$ at the short period and $S_1 = 0.6g$ at the 1-second period. The seismic weights were determined to be 5,992 kN for each typical floor and 5,284 kN for the roof. The study frames were designed for two seismic hazard levels: the maximum considered earthquake (MCE), which corresponds to a 2% probability of exceedance in 50 years, and the design basis earthquake (DBE), which corresponds to a 10% probability of exceedance in 50 years and is defined as two-thirds of the MCE intensity. The design base shear and the corresponding key design parameters are summarized in Table 2.

It is noted that yield drift (θ_y) was set to be 0.7%, while the target drift (θ_t) was specified as 2% for the DBE hazard level and 3% for the MCE hazard level. The design base shear coefficients (V_y/W) calculated using Eq. (8), were 0.164, 0.085, 0.057, and 0.045 for the 3-, 6-, 9-, and 12-story frames, respectively. The BRBs were installed at an inclination angle of 45° with respect to the adjacent beam-column connection, with a length ratio of $l_{bk}/l_b = 0.167$. The selected beam and column sections, together with the required BRB capacities for each frame, are summarized in Table 3. ASTM A36 steel (F_y = 248 MPa) was utilized for beams, columns, and BRB cores.

Table 2 Key EBPD parameters of the 3-, 6-, 9-, and 12-story D-BRKBF systems

Parameter	3-story		6-story		9-story		12-story	
Seismic level	DBE	MCE	DBE	MCE	DBE	MCE	DBE	MCE
$T(s)$	0.73	0.73	1.28	1.28	1.77	1.77	2.23	2.23
$S_a(g)$	0.82	1.23	0.47	0.70	0.34	0.51	0.27	0.41
$\theta_y(\%)$	0.70	0.70	0.70	0.70	0.70	0.70	0.70	0.70
$\theta_u(\%)$	2.00	3.00	2.00	3.00	2.00	3.00	2.00	3.00
$\theta_p = \theta_t - \theta_y(\%)$	1.30	2.30	1.30	2.30	1.30	2.30	1.30	2.30
$\mu = \theta_t/\theta_y$	2.85	4.28	2.85	4.28	2.85	4.28	2.85	4.28
R_μ	2.85	4.28	2.85	4.28	2.85	4.28	2.85	4.28
η	1.89	1.89	1.82	1.82	1.77	1.77	1.75	1.75
h^* (m)	9.52	9.52	18.36	18.36	27.40	27.40	36.55	36.55
γ_h	0.51	0.40	0.55	0.43	0.58	0.46	0.59	0.47
V_y/W	0.164	0.164	0.085	0.085	0.057	0.057	0.045	0.045

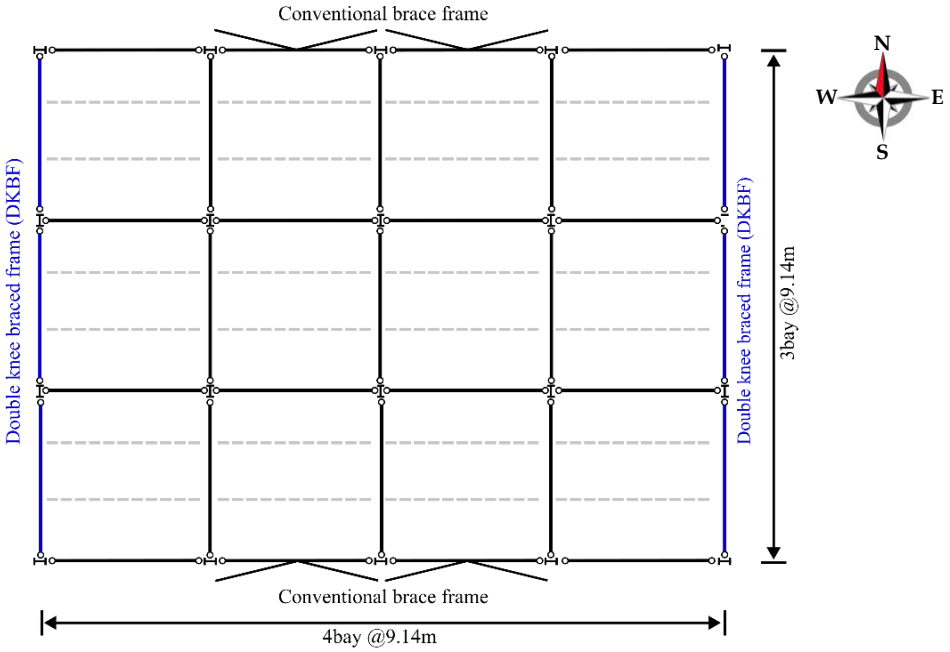

(a)

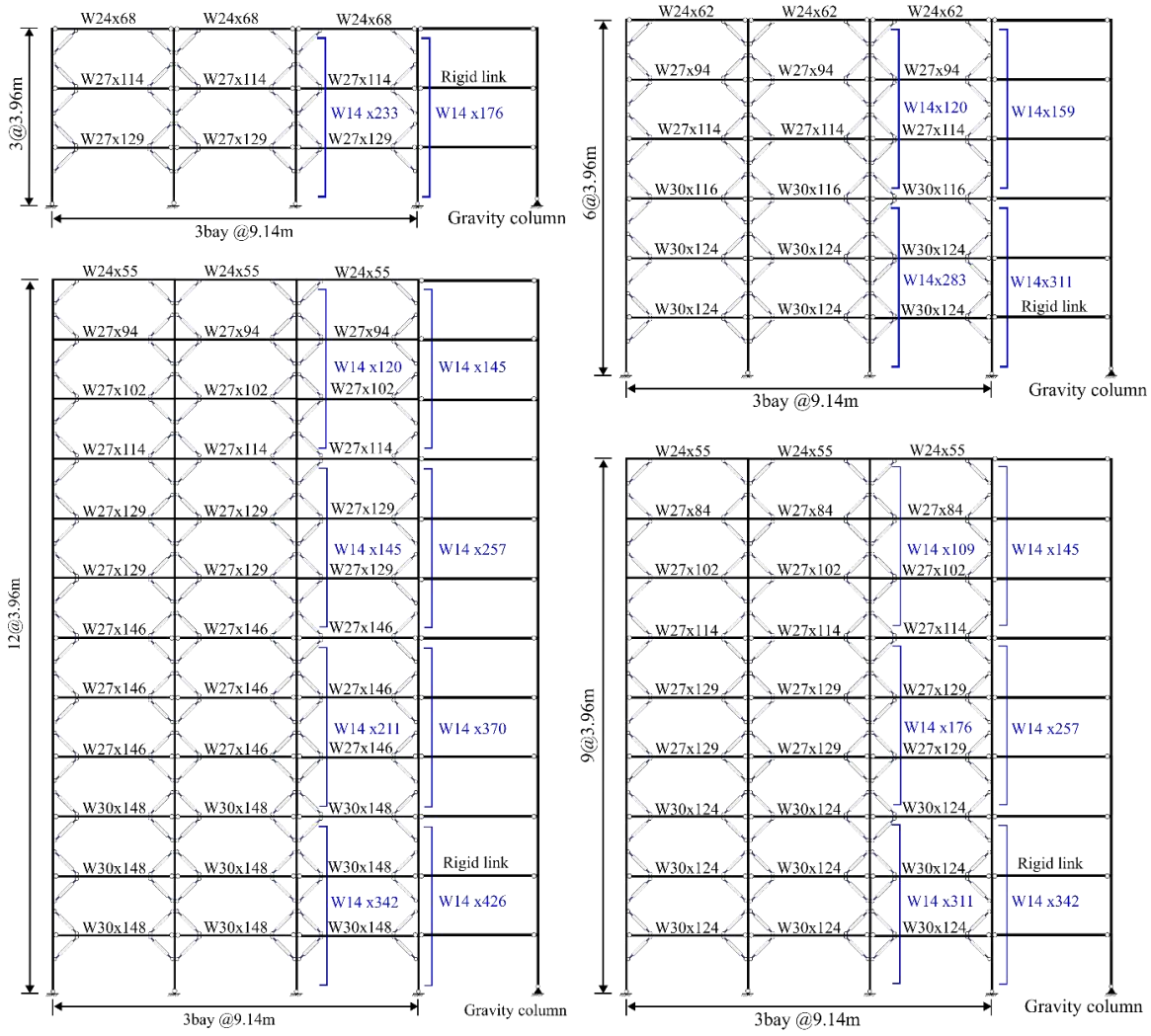

(b)

Fig. 7 Example 3-, 6-, 9-, and 12-story D-BRKBF systems: **(a)** plan view, and **(b)** 2D view

Table 3 Member sections based on the EBPD method

3-story D-BRKBF				
Story	BRBs capacity (kN)	Beam section	Column section	
		All bay	Interior	Exterior
1	455	W27x129	W14x233	W14x176
2	389	W27x114	W14x233	W14x176
3	248	W24x68	W14x233	W14x176
6-story D-BRKBF				
Story	BRBs capacity (kN)	Beam section	Column section	
		All bay	Interior	Exterior
1	490	W30x124	W14x283	W14x311
2	473	W30x124	W14x283	W14x311
3	438	W30x116	W14x283	W14x311
4	382	W27x114	W14x120	W14x159
5	302	W27x94	W14x120	W14x159
6	188	W24x62	W14x120	W14x159
9-story D-BRKBF				
Story	BRBs capacity (kN)	Beam section	Column section	
		All bay	Interior	Exterior
1	500	W30x124	W14x311	W14x342
2	493	W30x124	W14x311	W14x342
3	477	W30x124	W14x311	W14x342
4	453	W27x129	W14x176	W14x257
5	421	W27x129	W14x176	W14x257
6	378	W27x114	W14x176	W14x257
7	324	W27x102	W14x109	W14x145
8	258	W27x84	W14x109	W14x145
9	159	W24x55	W14x109	W14x145
12-story D-BRKBF				
Story	BRBs capacity (kN)	Beam section	Column section	
		All bay	Interior	Exterior
1	514	W30x148	W14x342	W14x426
2	510	W30x148	W14x342	W14x426
3	501	W30x148	W14x342	W14x426
4	488	W27x146	W14x211	W14x370
5	470	W27x146	W14x211	W14x370
6	448	W27x146	W14x211	W14x370
7	419	W27x129	W14x145	W14x257

8	385	W27x129	W14x145	W14x257
9	343	W27x114	W14x145	W14x257
10	292	W27x102	W14x120	W14x145
11	229	W27x94	W14x120	W14x145
12	145	W24x55	W14x120	W14x145

Performance evaluation

Structural modeling and calibration

Structural modeling, together with nonlinear static pushover (NSP) and nonlinear dynamic time-history (NDTH) analyses, was performed using the PERFORM-3D program. The D-BRKBF systems were modeled as two-dimensional (2D) frames with the P-Δ effects taken into account. To represent the gravity load-resisting system, a gravity column connected to the D-BRKBF through a rigid beam was incorporated into the analytical model. The boundary conditions were defined by fixing all column bases, except for the gravity column base, which was modeled as a pinned support. The seismic masses were lumped at the beam-column connections, while out-of-plane displacements were restrained. Gravity loads were modeled as concentrated nodal loads applied to the beams and columns. The nonlinear beam and column models were developed in accordance with FEMA 356 (2000) and calibrated against available experimental data. The BRBs were modeled as inelastic elements using a trilinear force-deformation relationship. The yielding core length of the BRBs was assumed to be 70% of the total brace length, following the modeling approach proposed by Sahoo and Chao (2010). The BRB model was calibrated against the experimental results of the subassembly tests reported by Junda et al. (2018). Two test specimens with different beam-column connection details, namely a pinned connection and a single-plate shear connection (SPSC), were considered for the calibration. The analytical results showed good agreement with the corresponding experimental responses for both connection types, as illustrated in Fig. 8.

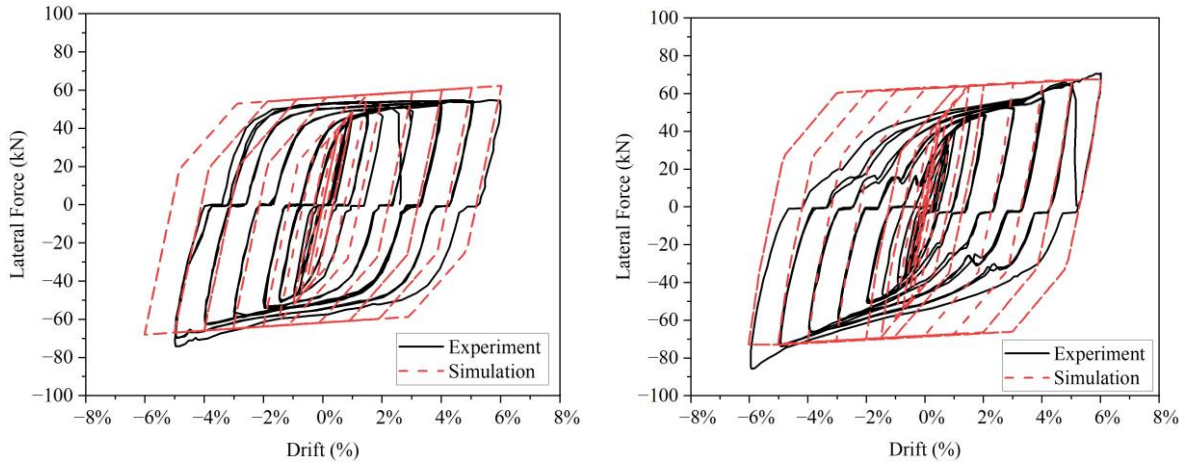

Fig. 8 Calibration of the BRB: analytical model against experimental results: **(a)** pinned connection specimen, and **(b)** single-plate shear connection (SPSC) specimen

Pushover analysis

A nonlinear static pushover analysis was conducted by incrementally applying lateral loads corresponding to increasing roof displacements, following a predefined lateral force distribution pattern. The pushover analysis was used to evaluate the inelastic response of the structure, including inelastic behavior and the failure mechanisms of the studied frames. Fig. 9 presents the pushover capacity curves of the 3-, 6-, 9-, and 12-story D-BRKBF systems. The capacity curves describe the relationship between the base shear coefficient and roof drift of the D-BRKBF systems. It was observed that the BRB members began to yield at approximately 0.17%, 0.30%, 0.31%, and 0.40% roof drift for the 3-, 6-, 9-, and 12-story frames, respectively. In contrast, yielding of the columns initiated at roof drifts of 1.34%, 1.69%, 2.22%, and 3.16% for the 3-, 6-, 9-, and 12-story frames, respectively. Fig. 10 illustrates the inelastic states of key structural components, such as BRBs and column bases, at a 2.0% roof drift obtained from the pushover analysis. It should be noted that the designated yielding members, including the BRBs and

column bases of the 3- and 6-story D-BRKBF systems, reached their inelastic states and achieved the intended plastic mechanism as designed. However, only BRB yielding was observed in the 9- and 12-story high-rise D-BRKBF systems at a 2% roof drift. This behavior may be attributed to higher-mode effects, which influence the relationship between roof drift and the target drift of the structure.

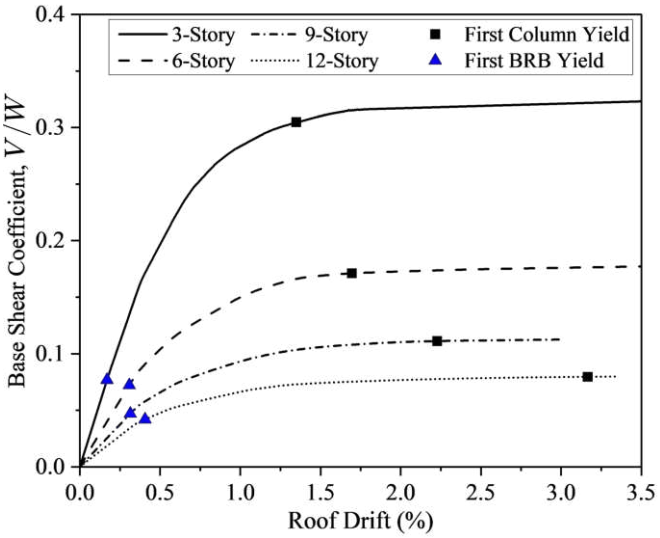

Fig. 9 Pushover capacity curves of the example D-BRKBF systems

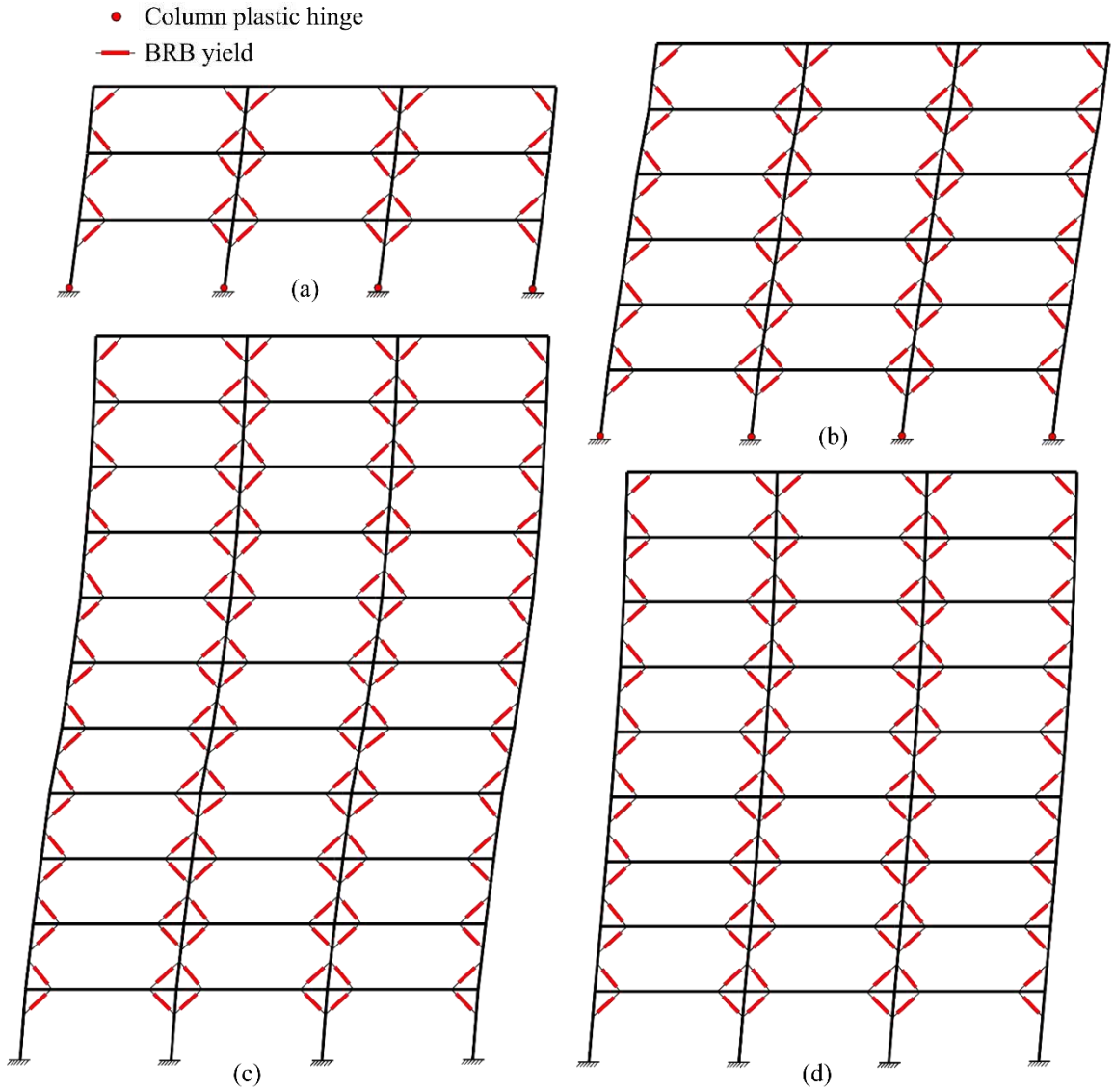

Fig. 10 Inelastic activities at 2% roof drift of pushover analysis: **(a)** 3-story D-BRKBF, **(b)** 6-story D-BRKBF, **(c)** 9-story D-BRKBF, and **(d)** 12-story D-BRKBF

Nonlinear dynamic time-history analysis

For the nonlinear dynamic time-history (NDTH) analyses, 22 pairs of far-field ground motion records with two horizontal components were selected. The ground motions were obtained from the PEER NGA-West2 database (PEER, 2023) in accordance with the recommendations of FEMA P695 (2009). The selected far-field record set has an average moment magnitude of $M_w = 7.0$, with magnitudes ranging from $M_w = 6.5$ to $M_w = 7.6$. The average source-to-site distance is 16.4 km, with a maximum distance of 26.4 km and a minimum distance of 11.1 km. The ground motions were amplitude-scaled to match the design response spectrum at the fundamental period of each study frame, as illustrated in Fig. 11.

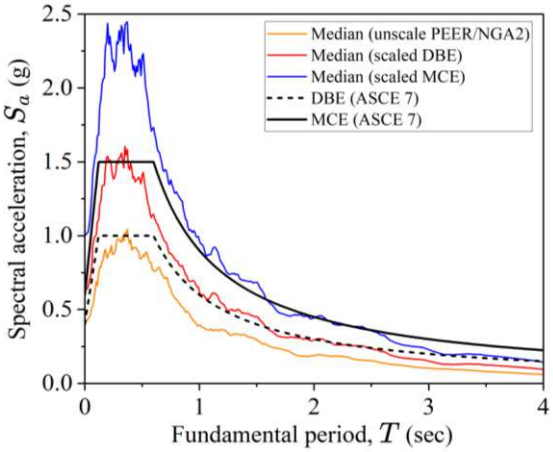

Fig. 11 Scaled median spectral accelerations

Figs. 12-15 illustrate the inelastic responses of the D-BRKBF systems under the selected ground motion records that produced inter-story drift ratios closest to the median values at the DBE and MCE hazard levels. In all cases, the column base plastic rotations and BRB plastic strain demands remained below the assumed deformation capacities of the corresponding members. At the DBE level, the BRB plastic strains remained below 1.0%, while the column base plastic rotations were less than 0.5% for all study frames. At the MCE level, the BRB plastic strains increased in the 3-story frame, with the upper-story BRBs reaching 1.0-2.0% and the lower-story BRBs remaining below 1.0%. In the 6- and 9-story frames, the BRB plastic strains were generally within the range of 1.0-2.0% at the upper and middle stories. In the 12-story frame, only several BRBs located at the third and fourth stories experienced plastic strains between 1.0% and 2.0%. The column base plastic rotations at the MCE level reached 1.0-1.5% and 0.5-1.0% for the 3- and 6-story frames, respectively. In contrast, the column base plastic rotations of the 9- and 12-story frames remained below 0.5%.

The estimated inter-story drift responses obtained from the nonlinear time-history analysis (NLTHA) using 22 pairs of ground motions are presented in Figs. 16 and 17. The results demonstrate that the median maximum inter-story drifts remained well within the predefined target drift limits of 2% for the DBE level and 3% for the MCE level for all D-BRKBF systems. Additionally, the inter-story drifts were observed to be well distributed in the low-rise D-BRKBF systems designed using EBPD. In the high-rise D-BRKBF systems, however, the story drift changed significantly at the lowest floor level due to the plasticity of the column bases.

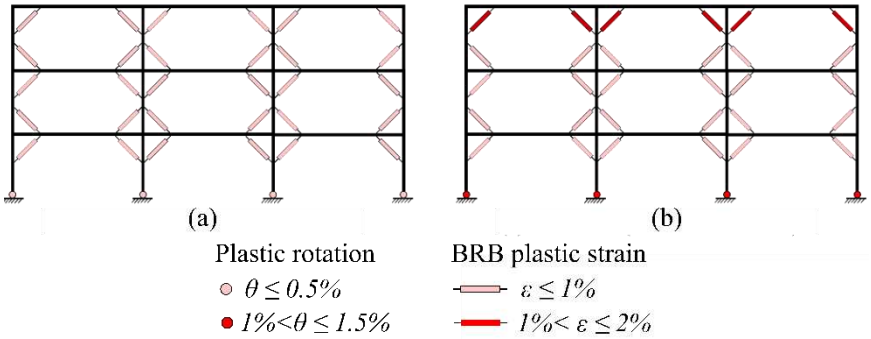

Fig. 12 Inelastic activity of a 3-story D-BRKBF system under NLHTA: **(a)** DBE level (SUPERT/B-POE360), and **(b)** MCE level (CHICHI/TCU045-N)

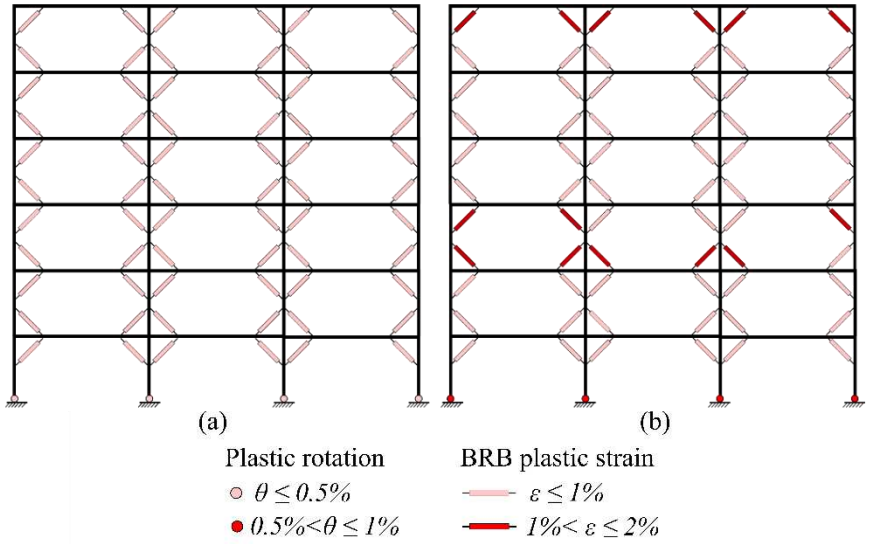

Fig. 13 Inelastic activity of a 6-story D-BRKBF system under NLHTA: **(a)** DBE level (FRIULI/A-TMZ000), and **(b)** MCE level (SUPERST/B-POE270)

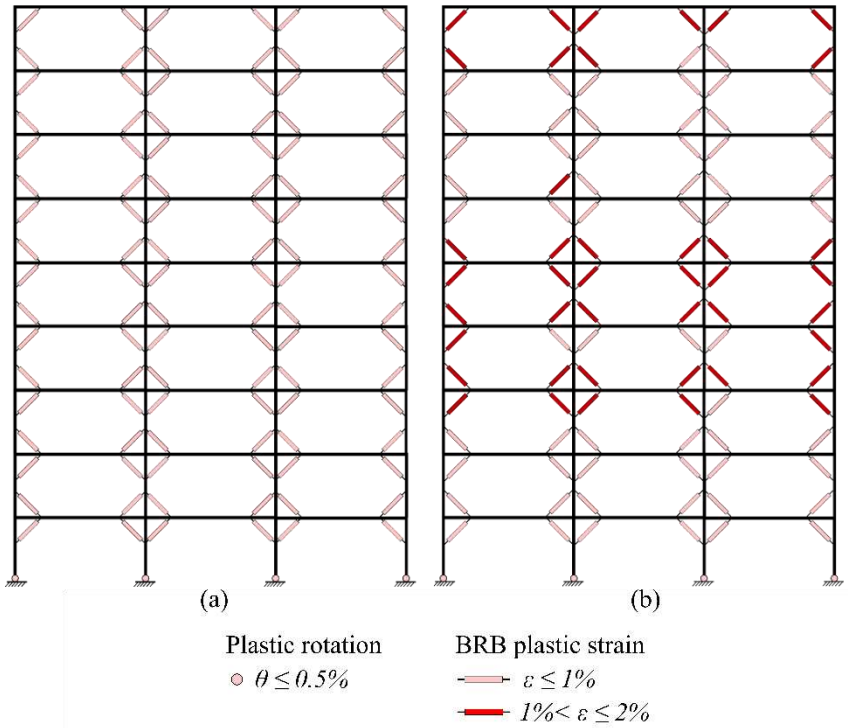

Fig. 14 Inelastic activity of a 9-story D-BRKBF system under NLHTA: **(a)** DBE level (IMVALL/H-E11230), and **(b)** MCE level (IMVALL/H-E11230)

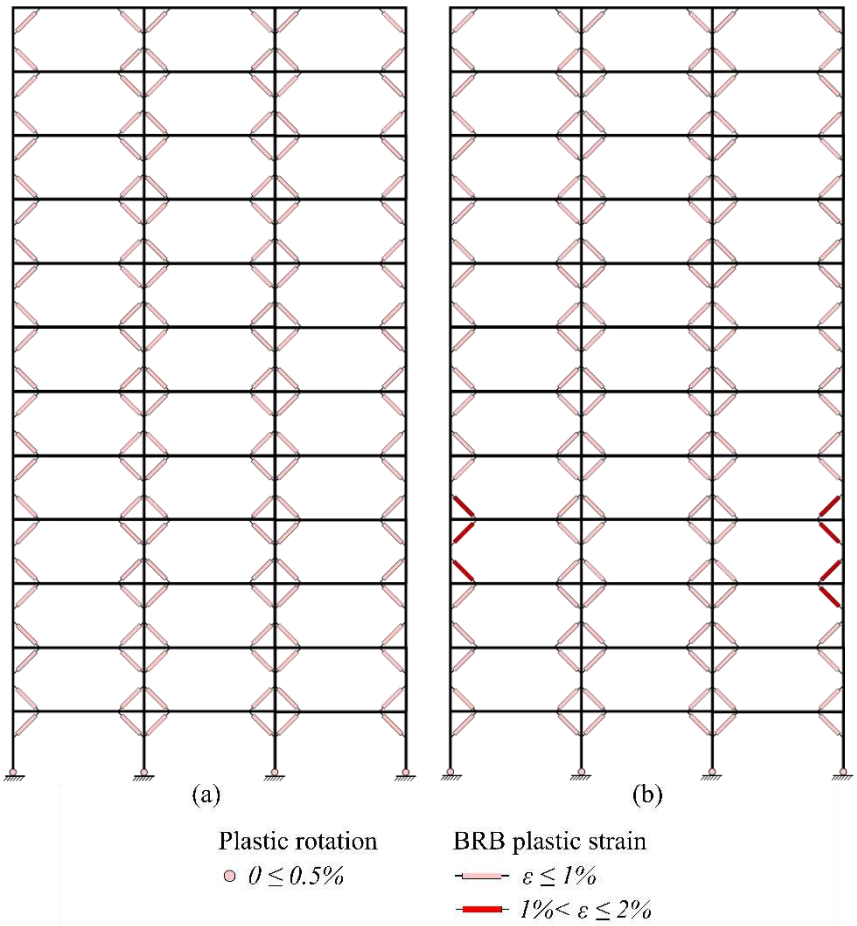

Fig. 15 Inelastic activity of a 12-story D-BRKBF system under NLHTA: **(a)** DBE level (SUPERST/B-IC00), and **(b)** MCE level (CHICHI/TCU045-E)

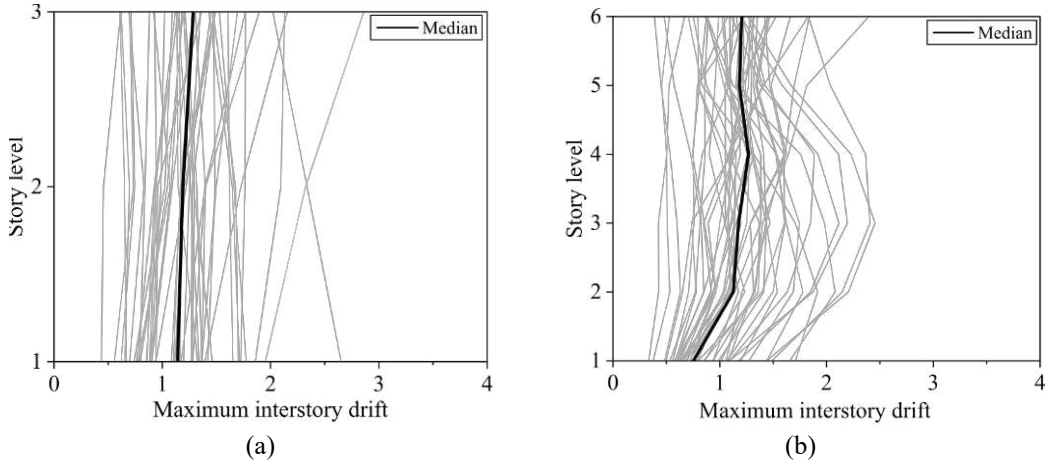

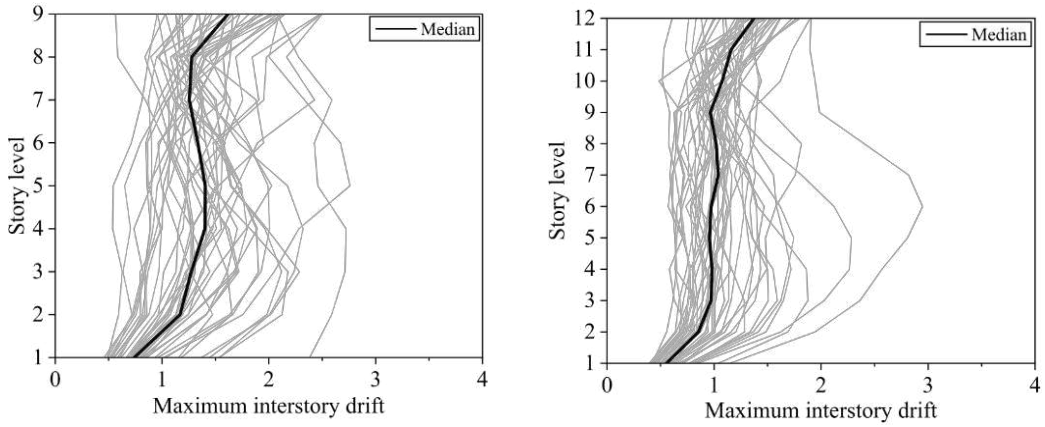

Fig. 16 Inter-story drift ratios obtained from the NLTHA at the DBE: **(a)** 3-story D-BRKBF, **(b)** 6-story D-BRKBF; (c) 9-story D-BRKBF, and (d) 12-story D-BRKBF

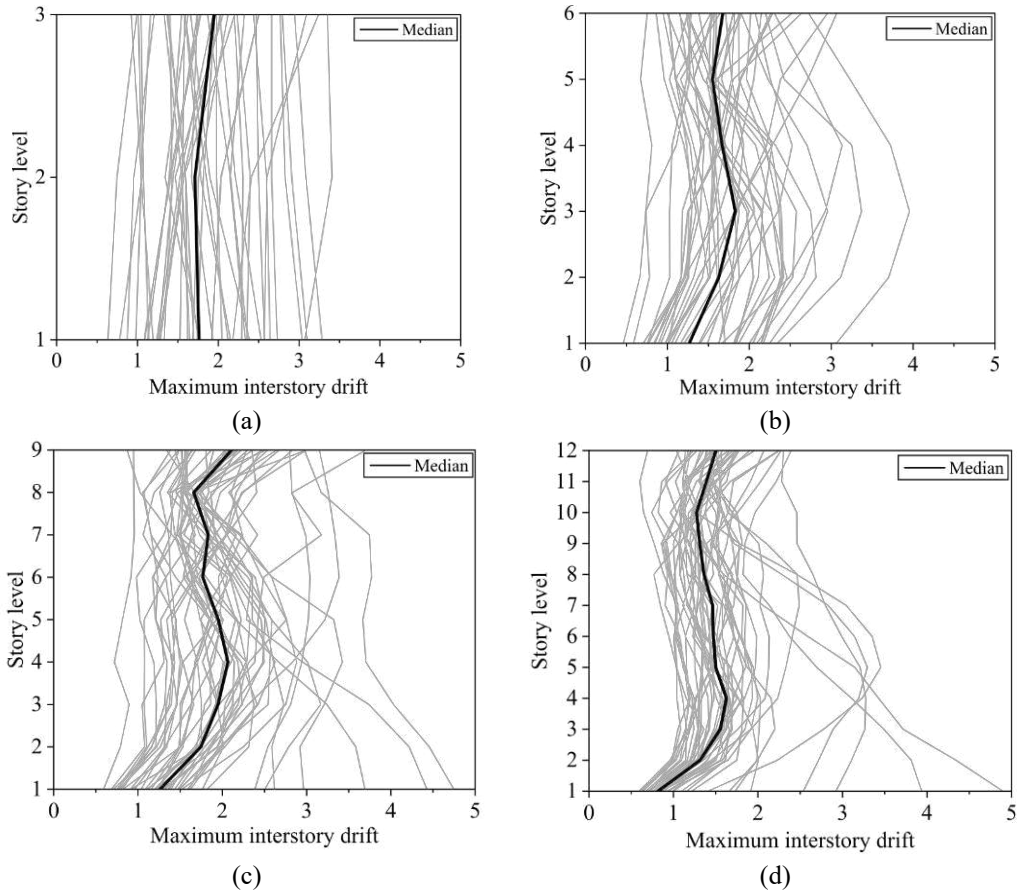

Fig. 17 Inter-story drift ratios obtained from the NLTHA at the MCE level: **(a)** 3-story D-BRKBF, **(b)** 6-story D-BRKBF, **(c)** 9-story D-BRKBF, and **(d)** 12-story D-BRKBF

Conclusions

This study presented the seismic design of doubly buckling-restrained knee-braced frame (D-BRKBF) systems equipped with buckling-restrained braces (BRBs) using the energy-based plastic design (EBPD) methodology. The EBPD approach was applied to calculate the design base shear of D-BRKBF systems with 3, 6, 9, and 12 stories under the design basis earthquake (DBE) and maximum considered earthquake (MCE) hazard levels. This base shear was then distributed over the height of the frame following the predefined yield mechanism. The structural member sizes were estimated using the capacity design. Seismic performance was evaluated with nonlinear static pushover (NSP) and nonlinear dynamic time-history (NDTH) analyses. The main findings are summarized as follows.

- The EBPD method is effective and applicable for the proposed D-BRKBF systems, especially for low- and medium-rise buildings. Both the NSP and NDTH analyses confirmed that yielding occurred predominantly in the designated yielding members.
- The proposed yield mechanism was fully achieved in the 3- and 6-story D-BRKBF systems within the target drift ratios of 2% and 3% at the DBE and MCE hazard levels, respectively. In addition, the median maximum inter-story drifts obtained from the NDTH analyses remained below the target drift limits set in the EBPD procedure.
- In the 9- and 12-story D-BRKBF systems, the proposed yield mechanism was not fully developed, as observed in the NSP analyses. The column bases did not yield within the target drifts predefined in the design, indicating the need for further study on the effects of higher-mode responses on the yield mechanism, especially with respect to the target drift. Nonetheless, the NDTH analyses showed that the 9- and 12-story D-BRKBF systems developed yielding in both the BRBs and the column bases within the target drift ratios of 2% and 3% at the DBE and MCE hazard levels, respectively.

In summary, the proposed EBPD framework provides a rational and effective seismic design method for low- and medium-rise D-BRKBF systems by ensuring controlled energy dissipation and the intended yield mechanism. Nevertheless, further studies are needed on high-rise D-BRKBF systems (more than six stories), with particular emphasis on the effects of higher-mode responses on the yield mechanism and the cumulative behavior under earthquake loading.

Acknowledgements

This research is collaboratively supported by the Research and Innovation Center of the Institute of Technology of Cambodia and the Department of Civil Engineering of the King Mongkut's University of Technology Thonburi.

References

AISC (ed.) (2010), *Seismic Provisions for Structural Steel Buildings*, American Institute of Steel Construction.

Alıcı FS and Sucuoğlu H (2016), "Prediction of input energy spectrum: attenuation models and velocity spectrum scaling," *Earthquake Engineering & Structural Dynamics*, **45**(13): 2137–2161. https://doi.org/10.1002/eqe.2749

ASCE/SEI (ed.) (2016), *Minimum design loads and associated criteria for buildings and other structures*, American Society of Civil Engineers, Reston, Virginia.

Chao S-H and Goel SC (2006), "Performance-Based Seismic Design of Eccentrically Braced Frames Using Target Drift and Yield Mechanism as Performance Criteria," *Engineering Journal*, **43**(3): 173–200. https://doi.org/10.62913/engj.v43i3.1294

Chea L, Doung P and Leelataviwat S (2025a), "Energy Demand and Damage Assessment of a Multi-Story Frame Based on Static Pushover Analysis," in Dindar AA, Benavent-Climent A, Mollaioli F and Varum H (eds.) *Energy-Based Seismic Engineering*, Springer Nature Switzerland, Cham, 304–315. https://doi.org/10.1007/978-3-031-97129-7_24

Chea L, Doung P and Leelataviwat S (2025b), "Energy-based plastic design of steel moment resisting frames considering cumulative damage," *Journal of Building Engineering*, **113**: 113831. https://doi.org/10.1016/j.jobe.2025.113831

Eknara Junda (2011), "Dynamic response of Knee-Braced moment Frames with partially restrained connections under earthquake excitations". https://doi.org/10.13140/RG.2.2.17272.15362

FEMA 356 (2000), "Prestandard and commentary for the seismic rehabilitation of buildings," *Federal Emergency Management Agency, Washington DC, USA*, .

FEMA P695 (2009), "Quantification of Building System Performance Factors," *Federal Emergency Management Agency, Redwood City, Washington D.C.*, .

Gao J, Xi J, Xu Y, Chen B, Zhao D, Zhao X and Chang Y (2022), "Mechanical Property of Beam-to-Column Connection of Steel Structures With All-Steel Buckling-Restrained Braces," *Frontiers in Materials*, **8**: 821299. https://doi.org/10.3389/fmats.2021.821299

Goel SC and Furukawa S (2009), "Role of Yield Mechanism Selection on Seismic Behavior of Steel Moment Frames Designed by Performance-Based Plastic Method," in *Structures Congress 2009*, American Society of Civil Engineers, Austin, Texas, United States, 1–9. https://doi.org/10.1061/41031(341)150

Goel SC, Liao W, Reza Bayat M and Chao S (2010), "Performance-based plastic design (PBPD) method for earthquake-resistant structures: an overview," *The Structural Design of Tall and Special Buildings*, **19**(1–2): 115–137. https://doi.org/10.1002/tal.547

Goudarzi SEM, Mortezaei A, Bitaraf A and Hemmati A (2026), "Development of an Energy-Based Damage Index for Moment-Resisting Reinforced Concrete Frame Structural System Under the Effect of Sequential Earthquakes," *Iranian Journal of Science and Technology, Transactions of Civil Engineering*, **50**(2): 1709–1735. https://doi.org/10.1007/s40996-025-01914-2

Housner GW (1956), “Limit Design of Structures to Resist Earthquakes,” *Proc. World Conference of Earthquake Engineering, 1956. 6*, . https://cir.nii.ac.jp/crid/1573387450439651200
Junda E, Leelataviwat S and Doung P (2018), “Cyclic testing and performance evaluation of buckling-restrained knee-braced frames,” *Journal of Constructional Steel Research*, **148**: 154–164. https://doi.org/10.1016/j.jcsr.2018.05.012
Kim J and Seo Y (2003), “Seismic design of steel structures with buckling-restrained knee braces,” *Journal of Constructional Steel Research*, **59**(12): 1477–1497. https://doi.org/10.1016/S0143-974X(03)00100-7
Leangheng C, Doung P and Leelataviwat S (2023), “Relation Between Input Energy and Equivalent Monotonic Response Curve,” in Varum H, Benavent-Climent A and Mollaioli F (eds.) *Energy-Based Seismic Engineering*, Springer Nature Switzerland, Cham, 87–97. https://doi.org/10.1007/978-3-031-36562-1_7
Lee S-S and Goel S (2001), *Performance-Based Design of Steel Moment Frames using Target Drift and Yield Mechanism*, Research Report UMCEE 01–17, Dept. of Civil and Environmental Engineering,University of Michigan, Ann Arbor, USA..
Leelataviwat S (1998), “Drift and yield mechanism based seismic design and upgrading of steel moment frames.,” University of Michigan.
Leelataviwat S, Doung P, Junda E and Chan-anan W (2019), “Ductile Knee-Braced Frames for Seismic Applications,” in Rupakhety R, Olafsson S and Bessason B (eds.) *Proceedings of the International Conference on Earthquake Engineering and Structural Dynamics*, Springer International Publishing, Cham, 149–158. https://doi.org/10.1007/978-3-319-78187-7_12
Leelataviwat S, Doung P and Naiyana N (2021), “A Review on Performance-Based Plastic Design Method: Concept and Recent Developments,” in Benavent-Climent A and Mollaioli F (eds.) *Energy-Based Seismic Engineering*, Springer International Publishing, Cham, 103–116. https://doi.org/10.1007/978-3-030-73932-4_8
Leelataviwat S, Saewon W and Goel SC (2009), “Application of Energy Balance Concept in Seismic Evaluation of Structures,” *Journal of Structural Engineering*, **135**(2): 113–121. https://doi.org/10.1061/(ASCE)0733-9445(2009)135:2(113)
Leelataviwat S, Suksan B, Srechai J and Warnitchai P (2011), “Seismic Design and Behavior of Ductile Knee-Braced Moment Frames,” *Journal of Structural Engineering*, **137**(5): 579–588. https://doi.org/10.1061/(ASCE)ST.1943-541X.0000301
Li J, Wang W and Li P (2021), “Development, testing and performance evaluation of steel beam-through framed connections with curved knee braces for improving seismic performance,” *Journal of Constructional Steel Research*, **179**: 106552. https://doi.org/10.1016/j.jcsr.2021.106552
Liao W-C and Goel SC (2012), “PERFORMANCE-BASED PLASTIC DESIGN AND ENERGY-BASED EVALUATION OF SEISMIC RESISTANT RC MOMENT FRAME,” *Journal of Marine Science and Technology*, **20**(3). https://doi.org/10.51400/2709-6998.1808
Merritt S, Uang C-M and Benzoni G (2003), “Subassemblage Testing of Star Seismic Buckling Restrained Braces,” *Structural Systems Research Project, Rep. No. TR-2003/04, Univ. of California at San Diego, San Diego*, .
Naiyana N, Leelataviwat S and Hajirasouliha I (2025), “Performance-based seismic design of buckling−restrained knee−braced frames: Cumulative damage optimization and design lateral force distribution,” *Structures*, **78**: 109167. https://doi.org/10.1016/j.istruc.2025.109167
Naiyana N, Leelataviwat S and Limkatanyu S (2023), “Seismic design of buckling-restrained knee-braced frames considering cumulative damage,” *Advances in Structural Engineering*, **26**(13): 2390–2407. https://doi.org/10.1177/13694332231185608
Newmark NM and Hall WJ (1982), *Earthquake spectra and design*, Earthquake Engineering Research Institute, Berkeley, Calif..
PEER (ed.) (2010), *Guidelines for Performance-Based Seismic Design of Tall Buildings*, PEER Report 2010-05, Pacific Earthquake Engineering Research Center, University of California, Berkeley, CA.
PEER (ed.) (2023), “PEER NGA-West2 Ground Motion Database”. Available: https://ngawest2.berkeley.edu/
Piseth Doung (2016), “Seismic Collapse Evaluation of Buckling-Restrained Knee-Braced Frames with Single Plate Shear Connections”. https://doi.org/10.13140/RG.2.2.28179.73766
Sahoo DR and Chao S-H (2010), “Performance-based plastic design method for buckling-restrained braced frames,” *Engineering Structures*, **32**(9): 2950–2958. https://doi.org/10.1016/j.engstruct.2010.05.014
Wongpakdee N, Leelataviwat S, Goel SC and Liao W-C (2014), “Performance-based design and collapse evaluation of Buckling Restrained Knee Braced Truss Moment Frames,” *Engineering Structures*, **60**: 23–31. https://doi.org/10.1016/j.engstruct.2013.12.014
Yang TY, Li Y and Leelataviwat S (2014), “Performance-Based Design and Optimization of Buckling Restrained Knee Braced Truss Moment Frame,” *Journal of Performance of Constructed Facilities*, **28**(6): A4014007. https://doi.org/10.1061/(ASCE)CF.1943-5509.0000558

Statements & Declarations

Funding
The authors declare that no funds, grants, or other support were received during the preparation of this manuscript.

Competing Interests
The authors have no relevant financial or non-financial interests to disclose.

Author Contributions
Piseth Doung and Sutat Leelataviwat conceived the study. Piseth Doung developed the methodology, provided resources, and supervised the work. Kimtong Theng carried out the investigation and formal analysis. Kimtong Theng and Leangheng Chea prepared the visualizations. The first draft of the manuscript was written by Piseth Doung and Kimtong Theng. Piseth Doung, Leangheng Chea, and Sutat Leelataviwat reviewed and edited the manuscript. All authors read and approved the final manuscript.

Supplementary Files

This is a list of supplementary files associated with this preprint. Click to download.

- 2.GraphicalabstractImageAJCE.pdf